Effect of different desiccant bed designs in a desiccant column on dehumidification performance

Prueksa Sawardsuk[1], Jiraporn Sripinyowanich Jongyingcharoen[2], Ekkapong Cheevitsopon[1*]

(1. Department of Food Engineering, School of Engineering, King Mongkut's Institute of Technology Ladkrabang, Bangkok 10520, Thailand; 2. Department of Agricultural Engineering, School of Engineering, King Mongkut's Institute of Technology Ladkrabang, Bangkok 10520, Thailand)

Abstract: The main objective of this study was to develop a desiccant column with enhanced air dehumidification. Multilayer desiccant beds with and without air ducts were designed in the column. The desiccant material was silica gel. Air dehumidification characteristics and psychrometric properties of air of various desiccant bed designs were investigated. Dehumidification rate, percentage adsorbed water, desiccant column effectiveness of each design were evaluated at an air flow rate of 1.2 m^3 min^{-1}, where the control was a single layer packed bed design. Both kinds of multilayer bed designs (with and without air ducts) exhibited a significantly better dehumidification rate, percentage adsorbed water, and desiccant column effectiveness than the control. The experimental dehumidification psychrometric process was consistent with the theoretical adiabatic dehumidification process. The percentage dehumidification rate as time passed for every multilayer bed design was better than that of the control. The 15-layer bed design with air ducts exhibited the highest values of about 15.73 g water min^{-1} dehumidification rate, 51.59% dehumidification efficiency, and 0.998 desiccant column effectiveness. This design shows good dehumidification performance and can be simply applied to many processes requiring air dehumidification.

Keywords: air dehumidifier, desiccant column, multilayer desiccant bed, silica gel

Citation: **S.** Prueksa., J. S. Jongyingcharoen and E. Cheevitsopon. 2022. Effect of different desiccant bed designs in a desiccant column on dehumidification performance. Agricultural Engineering International: CIGR Journal, 24 (1):207-216.

1 Introduction

The general dehumidifier designs that have been long used in industrial and residential applications are desiccant column and desiccant wheel (Chang et al., 2004; Rady, 2009). Column design provides a greater dehumidification capacity than wheel design (Zouaoui et al., 2016a; Abou-Ziyan et al., 2017). It has been applied to several processes requiring dehumidified air such as food drying (Attkan et al., 2014; Jedlińska et al., 2019; Rashidi et al., 2021; and Shewale et al., 2021), fuel combustion (Kucuk et al., 2003), air conditioning (Yang et al., 2017), corrosion prevention in electronics industry, seed storage and pharmaceutical cleanrooms etc. (Munters Corporation, 2019). In selecting a proper desiccant, adsorbent-adsorbate pairs are considered. Silica gel and zeolite pairs have been long used as desiccant material in industrial and residential applications because of their good water adsorption capacity. When the desiccant

Received date: 2020-10-26 **Accepted date:** 2021-05-21

***Corresponding author: Ekkapong Cheevitsopon,** Ph.D., Assistant Professor of Department of Food Engineering, School of Engineering, King Mongkut's Institute of Technology Ladkrabang, Bangkok 10520, Thailand. Email: ekkapong.ch@kmitl.ac.th. Tel: +66 23298356, Fax: +66 23298356 ext. 13.

absorbs moisture for a period of time, its adsorption ability is reduced, and regeneration is needed to remove the absorbed moisture. Silica gel needs a lower regeneration temperature than zeolite does. Silica gel regeneration temperature is less than 100°C (Chang et al., 2005; Ramzy et al., 2010). Many researchers have developed different designs of desiccant bed to mainly improve its dehumidifier efficiency as well as to improve some of its characteristics such as high adsorption capacity, low pressure drop and shorter regeneration time.

The design of desiccant bed to reduce air humidity found in previous studies take many forms such as packed bed (Ramzy et al., 2011), hollow bed (Awad et al., 2008; Balthazar et al., 2019), multilayer bed (Abou-Ziyan et al., 2017) and multi-stage packed bed (Yang et al., 2017, 2018), etc. Desiccant-coated bed has been used to reduce air humidity in air conditioning systems (Chang et al., 2005; Shamim et al., 2018) By the hollow bed model, it was found that increasing the ratio of outer and inner diameters increased the dehumidification capacity (Awad et al., 2008). Reducing the bed thickness causes the pressure drop to be lower (Awad et al., 2008; Abou-Ziyan et al., 2017; Shamim et al., 2018) and has a positive effect on heat exchange during the regeneration process as well. Reduced bed thickness also reduces regeneration time (Chang et al., 2005). Additionally, Yang et al. (2018), Yeboah and Darkwa (2021) added a cooling unit to reduce the temperature of the desiccant bed from heat of adsorption during the adsorption process, which led to an increase in the adsorption rate of the desiccant. However, in the study of dehumidifier efficiency, the condition of the inlet air should be kept constant throughout the experimental process (Chang et al., 2005; Awad et al., 2008; Kabeel, 2009; Abou-Ziyan et al., 2017; and Yang et al., 2017).

Factors of inlet air that affect the performance of dehumidifier are the amount of water in the air, temperature, and velocity. The amount of water or the temperature of the inlet air increase result in reduced dehumidification capacity (Abou-Ziyan et al., 2017). As the inlet air velocity increases, the desiccant exposure time is less, and the dehumidification capacity is also reduced (Zouaoui et al., 2016b). These literatures were utilized for the design of dehumidifier in this research to increase the efficiency of air dehumidification.

However, a design with multilayers of solid desiccant and air ducts in the desiccant container has never been developed before. The objectives of this study were to develop and evaluate such designs. A design of multilayers of desiccant with no air duct and a packed bed design were compared to the developed design. Several properties of the outlet air of each design were monitored and determined.

2 Materials and methods

2.1 Experiment setup

Figure 1(a) shows the experimental set-up of the desiccant column test unit. The unit consists of two main components: the inlet air controller and the desiccant column. The inlet air controller is composed of a heater and a water spray chamber. It was used to control the properties of the inlet air prior to its flowing into the desiccant bed (Kabeel, 2009; Ramzy et al., 2013; Abou-Ziyan et al., 2017). For the desiccant column, it can be changed in any designs. In this study, the designs of the desiccant bed are shown in Figure 1(b). The diameter of every desiccant bed was 20 cm, with a sieve at the bottom of the container. The container of a desiccant bed was of 2 types: with air duct (A) and without air duct (B). The bed container with an air duct had a duct with a diameter of 2.54 cm to allow air to pass through and between the layers of desiccant bed. The ducts in the A container were on alternating left and right sides of the succeeding desiccant bed layers. Hence the air flow direction in the A container was a zigzag flow pattern. The multilayer desiccant bed column either had 5, 10 or 15 layers. Thus, silica gel was packed in the desiccant column in 6 different treatments including 5 layers with air duct (5A); 10 layers with air duct (10A); 15 layers with air duct (15A); 5 layers without air duct (5B); 10 layers without air duct (10B); and 15 layers without air duct (15B). Packed bed (C) was used as the control column. Commercial silica gel (2-4 mm diameter, Power dry, Thailand) was used as a desiccant. Prior to use, silica gel was dried at 120°C for 12 hours (Rady, 2009; Yang et al., 2018) and kept in a close chamber until use. The moisture content of the silica gel was determined with an infrared moisture analyser (MA45; Sartorius, Germany). All bed designs were filled with the same total quantity of silica gel at 1950 g. Silica gel was portioned out equally to each layer in a multilayer bed.

2.2 Experimental process

All desiccant bed designs dehumidified the inlet air under the same conditions. The humidity ratio of ambient air was adjusted to 22 g water kg^{-1} dry air by the inlet air controller. The temperature of the inlet air was controlled by a heater to be about 31°C. The inlet air was sucked into the desiccant column by a blower at an air flow rate of 1.2 m^3 min^{-1}. The air mass flow rate was calculated from the average air velocity in the inlet air duct (V) using Equation 1 (Abou-Ziyan et al., 2017).

$$\dot{m} = \rho A V \quad (1)$$

where $\dot{m}$ is the mass flow rate of air (kg dry air min^{-1}), ρ is the air density (kg dry air m^{-3}), A is the cross-sectional area of the inlet air duct (m^2), and V is the air velocity (m min^{-1}).

The relative humidity and temperature of the inlet and outlet air were monitored throughout the experiment with a temperature hygrometer (KT320; KIMO, France). The air dehumidification process or the desiccant adsorption process was totally run for 60 min. The experiments were conducted in Pathum Thani province, Thailand (latitude 14.0895252, longitude 100.5919529) from February to April 2019.

2.3 Evaluation of dehumidification performance

Dehumidification performance of the desiccant column was defined in terms of the rate and efficiency of air dehumidification. Dehumidification rate and dehumidification efficiency were calculated using Equations 2 and 3, respectively (Abou-Ziyan et al., 2017; Yang et al., 2017).

$$\textit{Dehumidification rate (g water min}^{-1}\textit{)} = \dot{m}\,(w_i - w_o) \quad (2)$$

$$\textit{Dehumidification efficiency (\%)} = \frac{w_i - w_o}{w_i} \times 100 \quad (3)$$

where $\dot{m}$ is the mass flow rate of air (kg dry air min^{-1}), and w_i and w_o are the humidity ratio of inlet air and outlet air (g water kg^{-1} dry air).

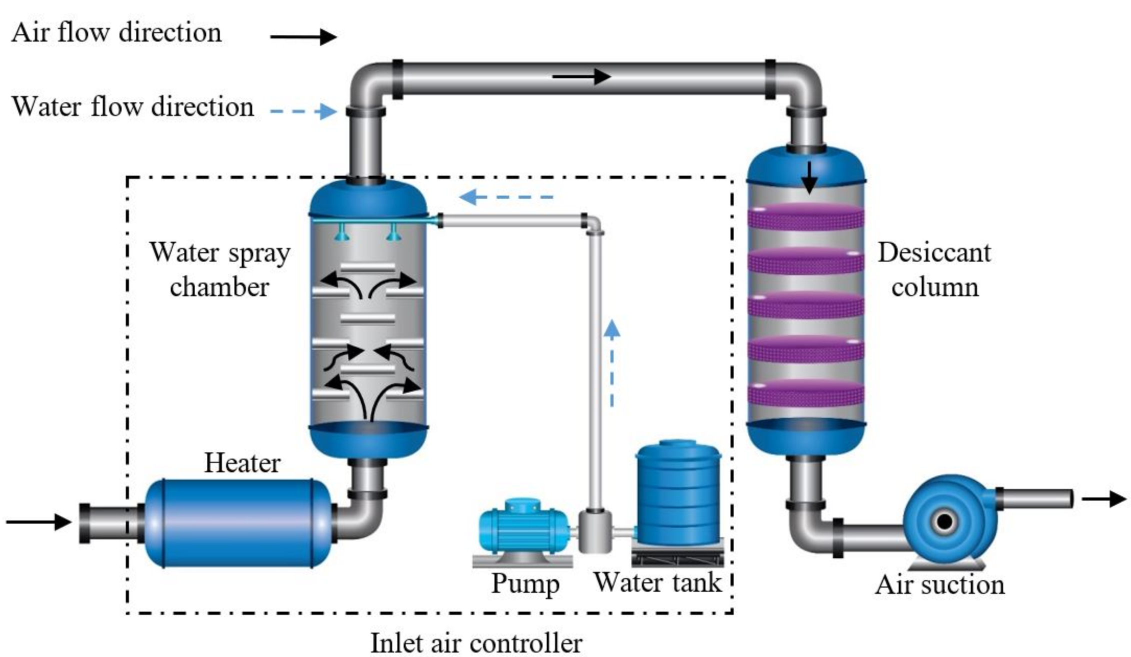

(a) The desiccant column test unit

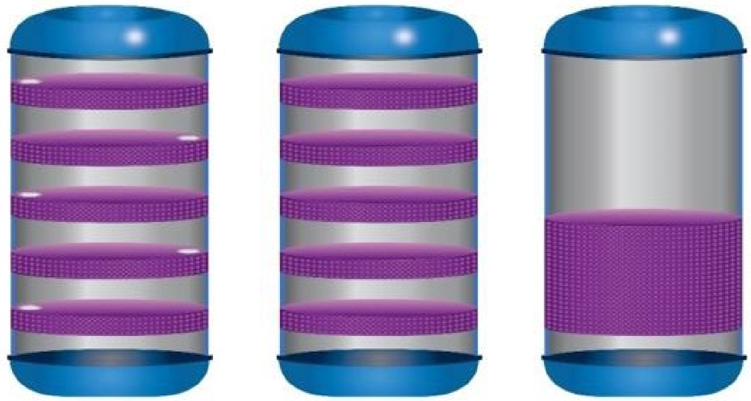

(b) The different desiccant bed designs of this study: multilayer bed with air duct (A); multilayer bed without air duct (B); and packed bed (C)

Figure 1 Schematic diagram of the desiccant column test unit

2.4 Analysis of psychrometric dehumidification process and effectiveness of the desiccant column

Dehumidification of air is an adiabatic process that is no change in heat content of air. However, deviation in the enthalpy could be observed. As described by Mandegari and Pahlavanzadeh (2009), this enthalpy deviation can be caused by isosteric heat, heat accumulation in a desiccant material and bed, and heat transfer from the regeneration process. In this way, the psychrometric process of air during the dehumidification was calculated. The effectiveness of the desiccant column was analyzed with respect to the enthalpy deviation from the adiabatic condition as in Equation 4 (Mandegari and Pahlavanzadeh, 2009; Suvanvisan et al., 2018). If the desiccant column was adiabatically operated, the effectiveness value would reach to 1.

$$\text{Desiccant column effectiveness}=1-\left|\frac{h_{out}-h_{ideal}}{h_{ideal}}\right| \quad (4)$$

where h_{out} is the enthalpy of outlet air (kJ kg^{-1} dry air), and h_{ideal} is the enthalpy of the adiabatic condition (kJ kg^{-1} dry air).

2.5 Statistical data analysis

The experiments were conducted in two replicates. The data were statistically analyzed by one-way analysis of variance (ANOVA) and Duncan's multiple range test at a significance level of 0.05.

3 Results and discussion

3.1 Dehumidified air characteristics

The incoming air prior pass through the desiccant column was adjusted to humidity ratio at 22 g water kg^{-1} dry air by air humidifier chamber. Figure 2 shows the variations in humidity ratio as time passed. At the beginning of the dehumidification process, the humidity ratio of the outlet air was the lowest because water vapor got adsorbed in the desiccant bed column during the system setup and the moisture content of the silica gel was at the lowest (Balthazar et al., 2019). The humidity ratio of the outlet air clearly and rapidly increased for the first 15 min. After that, the increase was gradual, but the humidity ratio of the outlet air was still lower than that of the inlet air as shown in Figure 2(a) and 2(b). Multilayer bed 15A was able to reduce the humidity ratio of inlet air by about 44% in the first minute and 15% in 30 min. Silica gel had a low moisture content at the beginning of the process and was able to adsorb a lot of moisture from the air. As time passed, its adsorption ability decreased and the humidity ratio of the exit air increased. The increasing humidity ratio of exit air with time follows the same trend as those observed in a packed bed, a thin-multilayer activated alumina bed, or a multilayer desiccant bed (Abou-Ziyan et al., 2017; Sawardsuk et al., 2018; Balthazar et al., 2020; Zallama et al., 2020).

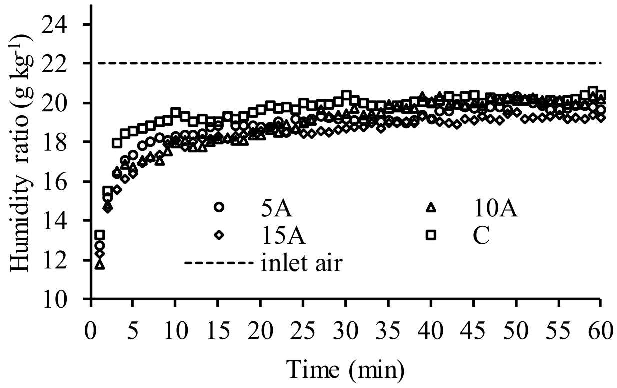

(a) Multilayer bed with air duct

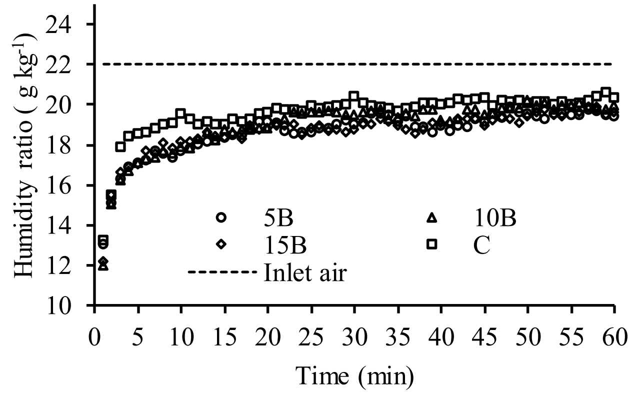

(b) Multilayer bed without air duct

Figure 2 Humidity ratio of outlet air versus dehumidification time of the desiccant column with different bed designs

Shown in Figure 3(a) and 3(b), the temperature difference between the inlet and outlet air at the start of the dehumidification process was small, then the outlet air temperature rose with time and reached the highest value at about 15 min after the start and then declined with time. The variation of the outlet air temperature followed the same trend as those observed in a packed bed or a radial flow bed (Awad et al., 2008; Ramzy et al., 2013; Zallama et al., 2020). The outlet air temperature during the first 15 min was higher than those of the rest of the dehumidification period. This was due to a higher amount of water vapor getting adsorbed in the initial period, which generated more heat of adsorption (Awad et al., 2008; Yeboah and Darkwa, 2021). This result agrees well with the low relative humidity of the exit air in the first 15 min. The maximum temperature difference between the outlet and inlet air was about 10°C.

3.2 Dehumidification rate

For every design of multilayer desiccant bed column, the dehumidification rate was the highest in the first minute, then it gradually decreased and plateaued out, as shown in Figure 4. The initial decreasing dehumidification rate with time was due to the increased moisture accumulation in silica gel (Zouaoui et al., 2016b). The difference in the dehumidification rates between that in the first minute and that at 30 min was about 10 g water min^{-1}. After 30 min, the dehumidification rate of every bed type stayed nearly constant. In Figure 4, it can be observed that the dehumidification rates of all multilayer bed columns were higher than that of the packed bed, at about 3 g water min^{-1}. The dehumidification rates of multilayer bed 15A and 15B were significantly higher than that of packed bed as shown in Figure 4(c) ($p \leq 0.05$). By the way, multilayer bed 15A gave the highest average dehumidification rate (Average dehumidification rate 15A 5.22 ± 2.18 g water min^{-1}, 15B 4.89 ± 2.04 g water min^{-1}). In dehumidification process by a desiccant column, the desiccant must be regenerated after it is used for a while. For 5-min dehumidification, the dehumidification rate of 15 layers columns was higher than that of a column with a fewer number of layers. Increasing the number of bed layers tended to increase the dehumidification rate. These results were like that of a thin-multilayer activated alumina bed type (Abou-Ziyan et al., 2017).

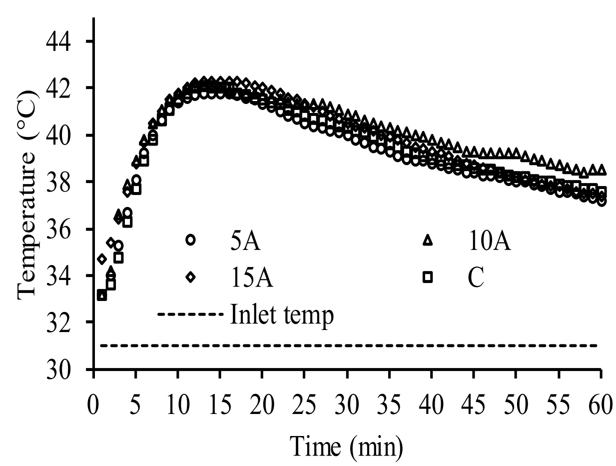

(a) Multilayer bed with air duct

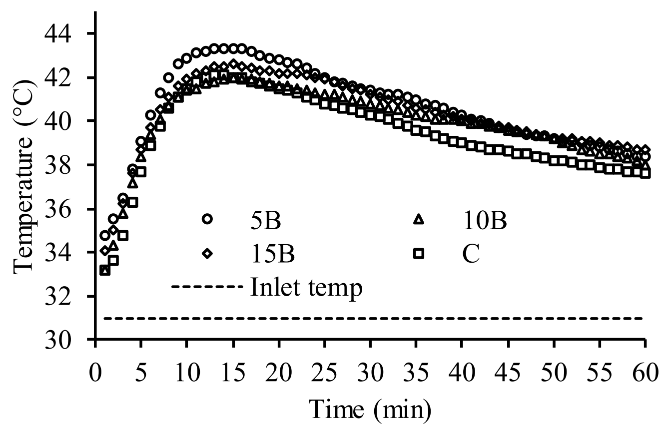

(b) Multilayer bed without air duct

Figure 3 Temperature of outlet air versus dehumidification time of the desiccant column with different bed designs

The multilayer bed type exhibited a lower value of the dehumidification rate reduction than the packed bed type did. It can be observed that, in the first 30 min, the dehumidification rate reduction differed clearly between the multilayer bed and packed bed types. At 60 min, the dehumidification rate reduction values of all type A beds were nearly the same. The number of layers had a slight influence on the dehumidification rate reduction. A low dehumidification rate reduction value resulted in a longer dehumidification process.

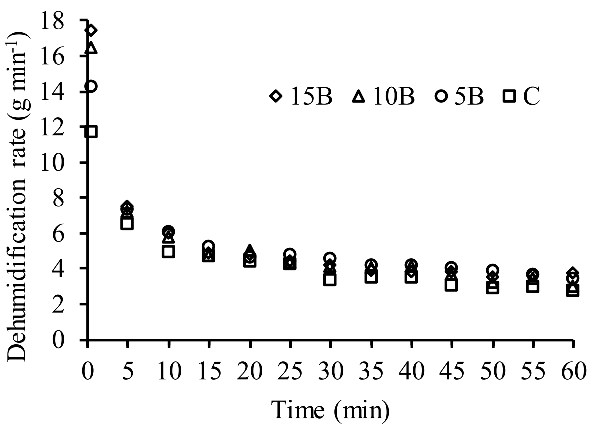

(a) Multilayer bed with air duct

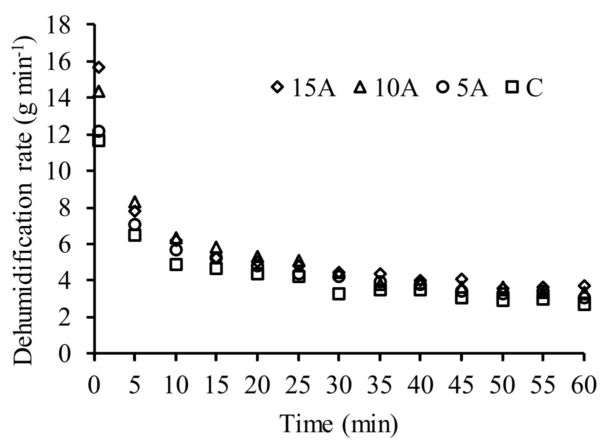

(b) Multilayer bed without air duct

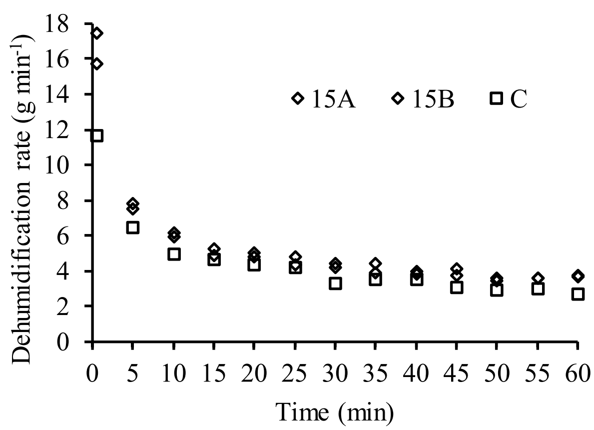

(c) 15 layers bed designs compare with control bed

Figure 4 Dehumidification rates of the desiccant column with different bed designs

3.3 Dehumidification efficiency

The amount of adsorbed water vapor was calculated from the difference between the humidity ratios of inlet and outlet air. Such percentage amount was defined as dehumidification efficiency. Figure 5 shows the effect of desiccant bed design on dehumidification efficiency for a period of 60 min. The dehumidification efficiency of every bed design followed the same trend. The dehumidification efficiency decreased with time during the first 30 min. After 30 min, the dehumidification efficiency remained almost constant. This result agrees with a finding from a study by Yang et al. (2017) that used silica gel to dehumidify air. In this study, multilayer bed 15A exhibited the highest dehumidification efficiency of 51.59% at the beginning of the dehumidification process. In addition, the average dehumidification efficiency was about 17%. The dehumidification efficiencies of all multilayer bed designs were higher than that of the packed bed design. The highest difference in dehumidification efficiency between bed 15A and bed C was 7.44%. At 60 min, the dehumidification rates for all bed types were nearly the same. The multilayer desiccant bed type 15A with air duct achieved a higher average efficiency than type 15B without air duct.

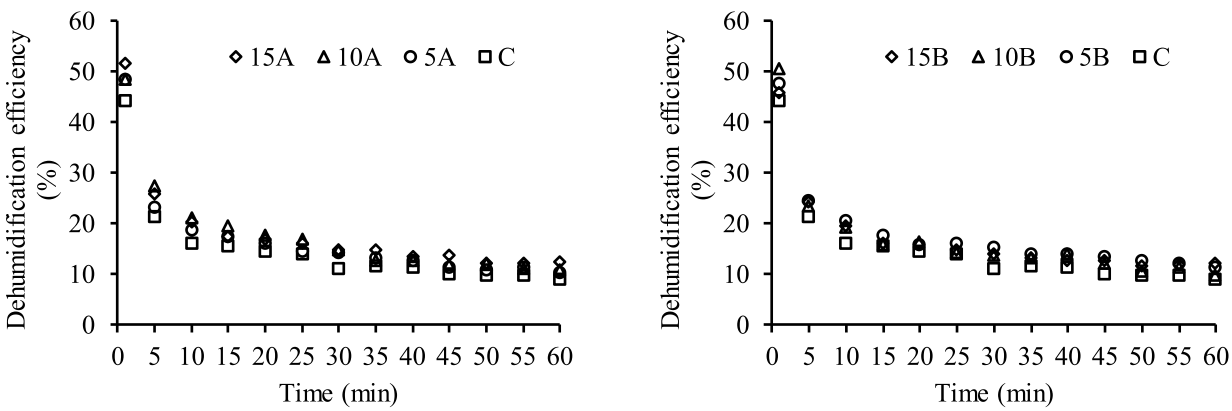

(a) Multilayer bed with air duct (b) Multilayer bed without air duct

Figure 5 Dehumidification efficiency of the desiccant column with different bed designs

3.4 Psychrometric dehumidification process and desiccant column effectiveness

Psychrometric dehumidification processes of the desiccant column with multilayer bed 15A at the dehumidification time of 1 min and 10 min are shown as representatives in Figure 6. The other bed designs exhibited the same trend of the dehumidification process on psychrometric chart. At the first minute of dehumidification, large variation was observed between the experimental and adiabatic process lines. As shown in the dehumidified air characteristics, the humidity ratio and temperature of the outlet air were both the lowest at the beginning. Heat of air was lost at this time with about 33 kJ kg^{-1} dry air reduction of enthalpy value. This could be the result of conduction heat transfer occurring between the desiccants themselves and between the desiccants and the walls of the column beds (Long and Guan, 2012) as the desiccants and the column was at ambient temperature during the first period of the process. Additionally, convective heat transfer between the desiccant column and process air considerably occurs during this period because of high temperature gradient (Laguerre et al., 2006). In contrast, after a 10-min operation, the outlet air was approximately at the highest temperature (see Figure 3) presenting that the heat of adsorption, which was generated by the desiccants, was not much transferred to the test unit. During this period, the experimental and adiabatic process lines were almost aligned.

Based on the variation of the experimental dehumidification process and the theoretical adiabatic dehumidification process, the desiccant column effectiveness was calculated for each desiccant bed design

(Figure 7). The effectiveness values were the lowest at the first minute and then raised to almost 1 and kept constant at the highest effectiveness for the rest of the process. The desiccant column effectiveness observed in this study was consistent with the desiccant effectiveness of desiccant wheel reported by Mandegari and Pahlavanzadeh (2009) and Suvanvisan et al. (2018).

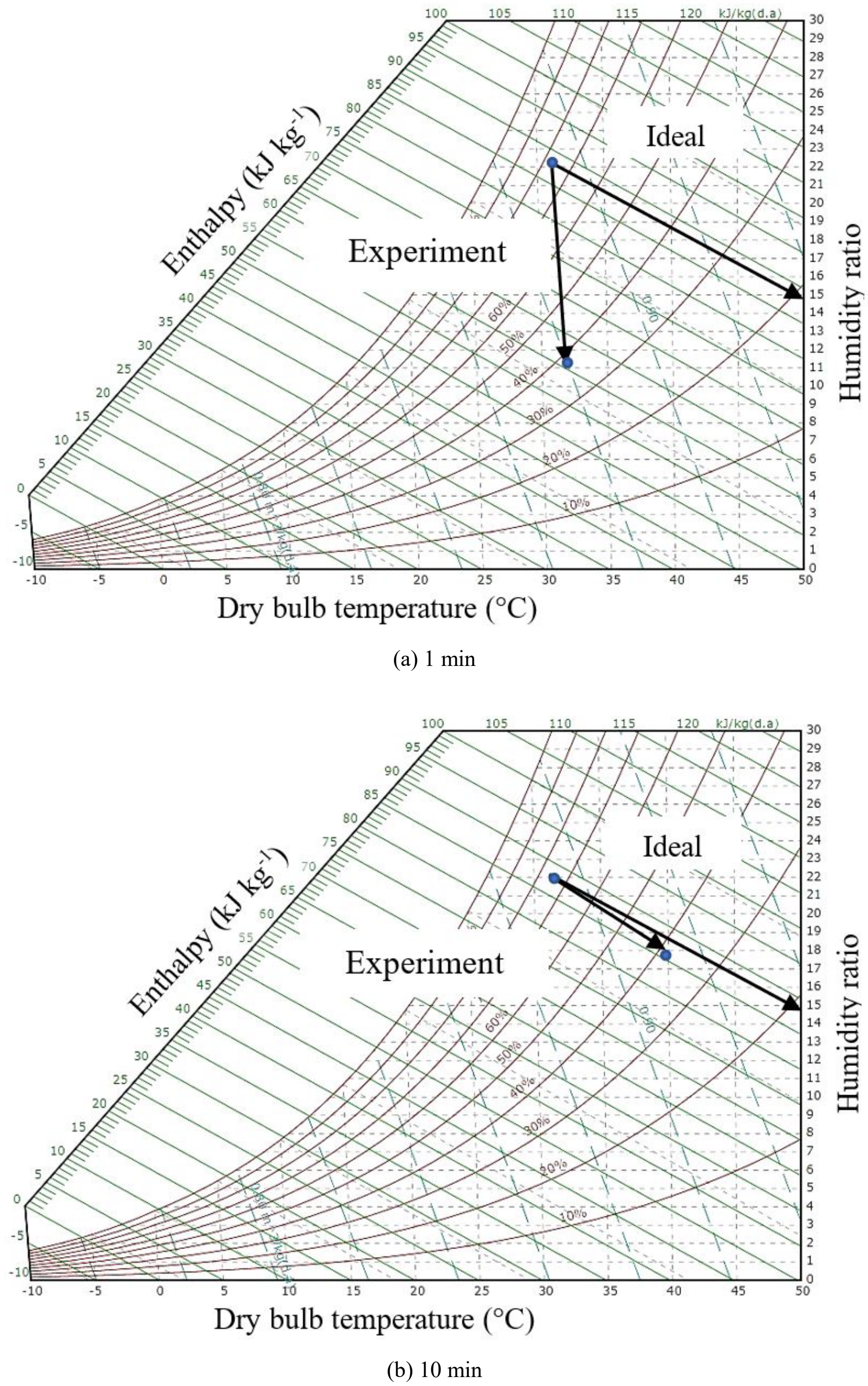

Figure 6 Representative psychrometric dehumidification process of the desiccant column with multilayer bed 15A. (Psychrometric Chart adapted from FlyCarpet Inc (2020))

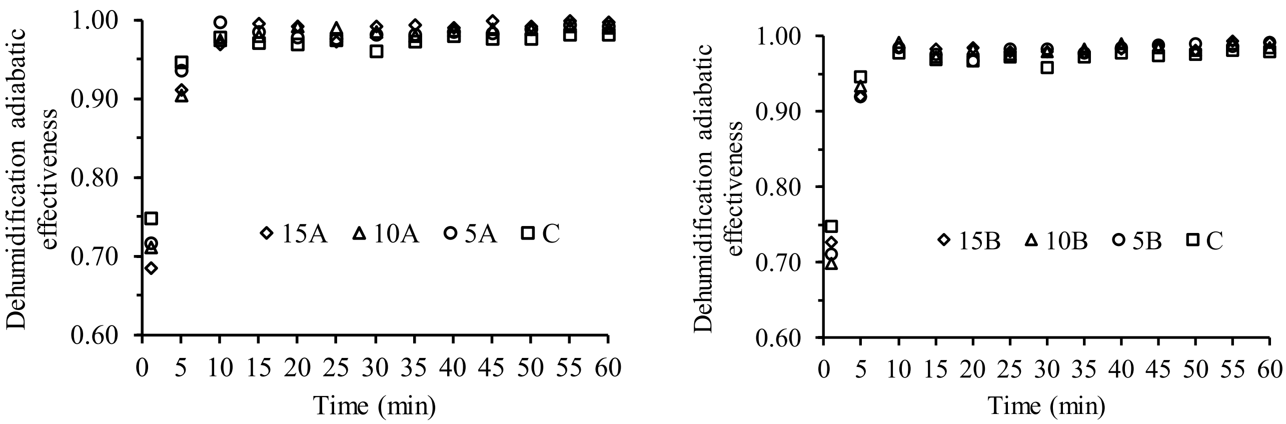

(a) Multilayer bed with air duct (b) Multilayer bed without air duct

Figure 7 Desiccant column effectiveness of the desiccant column with different bed designs

4 Conclusions

Various multilayer desiccant bed designs were evaluated. The dehumidified air reached the lowest humidity in the first minute; the outlet humidity ratio then increased slightly with time. The temperature difference between the inlet and outlet air could be as high as 10°C, a distinct benefit that reduces energy expenditure in drying food. The results show that different designs exerted different effects on dehumidification rate and dehumidification efficiency. A 15-layer desiccant column in a container with air duct design exhibited the highest average dehumidification rate, dehumidification efficiency, and desiccant column effectiveness of 15.73 g water min^{-1}, 51.59%, and 0.998, respectively. The main dehumidification period was 30-min long. Multilayer bed designs provided better results than the packed bed design. The dehumidification efficiency of the multilayer bed design was 7.44% higher than that of the packed bed design. Increasing the number of bed layers tended to increase dehumidification rate and dehumidification efficiency in a multilayer bed design. The experimental dehumidification process was aligned well adiabatic dehumidification process. The 15-layer desiccant bed with air duct design was better than other bed designs in terms of dehumidification rate and efficiency.

Acknowledgement

This research project was supported by the National Research Council of Thailand, fiscal year of 2016.

References

Abou-Ziyan, H., D. Abd El-Raheim, O. Mahmoud, and M. Fatouh. 2017. Performance characteristics of thin-multilayer activated alumina bed. *Applied Energy*, 190(c): 29-42.

Attkan, A. K., N. Kumar, and Y. K. Yadav. 2014. Performance evaluation of a dehumidifier assisted low temperature based food drying system. *IOSR Journal of Environment Science, Toxicology and Food Technology*, 8(1): 43-49.

Awad, M. M., A. K. Ramzy, A. M. Hamed, and H. M. Bekheit. 2008. Theoretical and experimental investigation on the radial flow desiccant dehumidification bed. *Applied Thermal Engineering*, 28(1): 75-85.

Balthazar, P., M. A. Ismail, L. C. Khai, M. I. Ramdan, N. M. Mazlan, and H. B. Mamat. 2019. Adsorption characteristic of a two layer hollow cylindrical silica bed. In *Proceedings of International Conference of Aerospace and Mechanical Engineering 2019*, 493-500. Penang, Malaysia, 20–21 November.

Balthazar, P., M. A. Ismail, M. N. M. Nasir, H. Mamat, and M. I. Ramdan. 2020. Experimental investigation on a desiccant silica bed for dehumidification. *Journal of Advanced Research in Fluid Mechanics and Thermal Sciences*, 73(2): 1-11.

Chang, S., H. Wang, and T. Chung. 2004. Effect of regeneration conditions on the adsorption dehumidification process in packed silica gel beds. *Applied Thermal Engineering*, 24(5-6): 735-742.

Chang, S., M. Chen, and T. Chung. 2005. Effect of the thickness and particle size of silica gel on the heat and mass transfer performance of silica gel-coated bed for air-conditioning adsorption systems. *Applied Thermal Engineering*, 25(14-15): 2230-2340.

FlyCarpet Inc. 2020. Free Online Interactive Psychrometric Chart. Available at: http://www.flycarpet.net/en/psyonline. Accessed 20 October 2020.

Jedlińska, A., K. Samborska, A. Wieczorek, A. Wiktor, E. Ostrowska-Ligęza, W. Jamróz, K. Skwarczyńska-Maj, D. Kiełczewski, L. Błażowski, M. Tułodziecki, and D. Witrowa-Rajchert. 2019. The application of dehumidified air in rapeseed and honeydew honey spray drying - Process performance and powders properties considerations. *Journal of Food Engineering*, 245: 80-87.

Kabeel, A. E. 2009. Adsorption - desorption operation of multilayer desiccant packed bed for dehumidification applications. *Renewable Energy*, 34(1): 255-265.

Kucuk, A., Y. Kadioglu, and M. S. Gulabglu. 2003. A study of spontaneous combustion characteristics of a Turkish lignite: particle size, moisture of coal, humidity of air. *Combustion and Flame*, 133(3): 255-261.

Laguerre, O., S. B. Amara, and D. Flick. 2006. Heat transfer between wall and packed bed crossed by low velocity airflow. *Applied Thermal Engineering*, 26(16): 1951-1960.

Long, X., and Y. Guan. 2012. Measurement of diffusivity and thermal parameters of gas adsorption with a volumetric method. *Industrial & Engineering Chemistry Research*, 51(18): 6502–12.

Mandegari, M. A., and H. Pahlavanzadeh. 2009. Introduction of a new definition for effectiveness of desiccant wheels. *Journal of Chemical Engineering*, 34(6): 797–803.

Munters Corporation. 2019. The Dehumidification Handbook. Available at: https://www.munters.com/globalassets/documents/airt/solutions/the-dehumidification-handbook---third-edition.pdf. Accessed 19th May 2021.

Rady, M. A. 2009. Experimental and numerical investigations on the performance of dehumidifying desiccant beds composed of silica-gel and thermal energy storage particles. *Heat Mass Transfer*, 45(5): 545-561.

Ramzy, A. K., A. M. Hamed, M. M. Awad, and M. M. Bekheit. 2010. Theoretical investigation on the cyclic operation of radial flow desiccant bed dehumidifier. *Journal of Engineering and Technology Research*, 2(6): 96-110.

Ramzy, A. K., R. Kadoli, and T. P. A. Babu. 2011. Improved utilization of desiccant material in packed bed dehumidifier using composite particles. *Renewable Energy*, 36(2): 732-742.

Ramzy, A. K., R. Kadoli, T. P. Ashok Babu. 2013. Experimental and theoretical investigation on the cyclic operation of TSA cycle for air dehumidification using packed bed of silica gel particles. *Energy*, 56: 8-24.

Rashidi, M., A. Arabhosseini, H. Samimi-Akhijahani, and A. M. Kermani. 2021. Acceleration the drying process of oleaster (Elaeagnus angustifolia L.) using reflectors and desiccant system in a solar drying system. *Renewable Energy*, 171(2): 526-541.

Shewale, S. R., D. Rajoriya, M. L. Bhavya, and H. U. Hebbar. 2021. Application of radiofrequency heating and low humidity air for sequential drying of apple slices: Process intensification and quality improvement. *LWT-Food Science and Technology*, 135(2): 109904.

Sawardsuk, P., J. S. Jongyingcharoen, and E. Cheevitsopon. 2018. Experimental investigation of air characteristics during dehumidification in the multilayer desiccant bed column system. In *MATEC Web of Conferences*, 192: 03012. Phuket, Thailand, 4-7 July.

Shamim, J., W. Hsu, K. Kitaoka, S. Paul, and H. Daiguji. 2018. Design and performance evaluation of a multilayer fixed-bed binder-free desiccant dehumidifier for hybrid air-conditioning systems: Part i-experimental. *International Journal of Heat and Mass Transfer*, 116(4A): 1361-1369.

Suvanvisan, P., E. Cheevitsopon, and J. S. Jongyingcharoen. 2018. Study on psychrometric properties of air in a hot air drying system combined with a desiccant wheel. *TSAE Journal*, 24(1): 6-12.

Yang, W., H. Deng, Z. Wang, X. Zhao, and S. He. 2017. Performance investigation of the novel solar-powered dehumidification window for residential buildings. *Energies*, 10(9): 1369.

Yang, W., J. Ren, Z. Lin, Z. Wang and X. Zhao. 2018. Study on dehumidification performance of a multi-stage internal cooling solid desiccant adsorption packed bed. *Energies*, 11(11): 3038.

Yeboah, S. K., and J. Darkwa. 2021. Experimental investigation into the integration of solid desiccant packed beds with oscillating heat pipes for energy efficient isothermal adsorption processes. *Thermal Science and Engineering Progress*, 21(14-15): 100791.

Zallama, B., L. Zili-Ghedira, and S. B. Nasrallah. 2020. Performance of a new desiccant bed using phase change material. In *MATEC Web Conference*, 330: 01015. Hammamet, Tunisia, 23-26 April.

Zouaoui, A., L. Zili-Ghedira, and S. B. Nasrallah. 2016a. Open solid desiccant cooling air systems: a review and comparative study. *Renew Sustain Energy*, 54: 889-917.

Zouaoui, A., L. Zili-Ghedira, and S. B. Nasrallah. 2016b. Experimental investigation of air dehumidification and regeneration operations using packed bed of silica gel particles. *International Journal of Heat and Technology*, 34(1): 103-109.